Adsorption 11: 91–96, 2005

Menisci Interactions during Adsorption on Mesoporous Materials: Evaluation of Delayed and Advanced Adsorption

SALOMON CORDERO, FERNANDO ROJAS,* ISAAC KORNHAUSER, AND MARCOS ESPARZA
Departamento de Química Universidad Autónoma Metropolitana-Iztapalapa, P.O. Box 55-534, México D.F. 09340, México

GIORGIO ZGRABLICH
Laboratorio de Ciencias de Superficies y Medios Porosos, Universidad Nacional de San Luis, San Luis, Argentina
fernando@xanum.uam.mx

Abstract. Menisci interactions can strongly affect the development of adsorption processes in mesoporous materials. Phenomena such as delayed and advanced adsorption represent outright manifestations of these interactions then leading to deceptive determinations of the pore-size distribution. At present, a characterization study involving simulated porous networks with qualities similar to those owned by real materials and in which the above processes can occur is still lacking. A Monte Carlo procedure is used to evaluate the extent of delayed and advanced adsorption in porous structures of assorted morphologies. This treatment allows a clear detection of the types of mesoporous structures that can experience the incidence of delayed and advanced adsorption.

Keywords: delayed adsorption, advanced adsorption, Monte Carlo simulation, porous networks

Introduction

When performing a sorption characterization analysis, the simultaneous incidence of varied phenomena usually renders an inappropriate assessment of the structural parameters of a porous material. Some of these perturbing phenomena can be related to the variation of the density of the adsorbed phase along the pore axes (Neimark, 1995), as well as to the magnitude of the potential field emanating from the pore walls towards the adsorbed molecules. Factors of this nature make difficult to calculate the correct conditions for a given pore to be occupied by condensate, especially in the nanopore size interval (Ravikovitch et al., 1997). Additionally, desorption conditions are also hard to evaluate by reason of two further phenomena: the classical pore-blocking effect and the more recent cavitation process. The pore-blocking effect consists in the impediment for a pore to evaporate its condensate if this void has no direct access to the vapor phase, thus turning evaporation from pore entities into a percolation process. Cavitation implies the possibility that a condensate-filled pore could turn empty by means of bubble nucleation within the condensed liquid. Cavitation studies carried out so far have been mostly focused upon ink-bottle pores and have suggested that sometimes the shape of the desorption isotherm is mainly dictated by this phenomenon rather than by the pore-blocking effect (Sarkisov and Monson, 2000).

In spite of the recognition of the above processes, up till now two additional phenomena have been mostly ignored: we call them "delayed" and "advanced" adsorption. Advanced adsorption describes the spontaneous liquid-filling that suffers a tubular capillary as a consequence of the irruption of an advancing liquid-vapor interface proceeding from an adjacent wider cavity; this irreversible liquid-filling occurs prior to the accomplishment of the limiting condition for a

*To whom correspondence should be addressed.

vapor-liquid transition to occur inside the isolated, unconnected tubular pore; this being the reason of the "advanced" labeling. Although advanced adsorption could become really relevant since it may sometimes trigger an avalanche liquid-filling of the pore network, only few authors have referred to it (e.g., Androutsopoulos and Salmas, 2000). In turn, delayed adsorption describes the filling of a wide pore with condensate once the thermodynamic metastability limit of the adsorbed film deposited on the walls of the void has been surpassed. This phenomenon is due to the existence of a discontinuous liquid-vapor interface around a pore cavity which prevents the movement of a unified liquid-vapor meniscus toward the center of the pore in question; this discontinuity is due to the presence of empty pores surrounding the cavity under analysis. This effect may also be rather relevant, but again only few authors have cared about it (Mayagoitia et al., 1985).

This work treats about delayed and advanced adsorption. Our goal is to propose a method to realize the veracity and virulence of each of the above processes in a given porous structure. We accomplish our objectives by simulating N_2 sorption isotherms at 77 K on Monte Carlo-generated 3-D porous networks.

Advanced Adsorption

Imagine a sinuous tubular capillary consisting of bulges and throats (see Fig. 1). Two main situations can arise (Everett, 1975). The first one concerns the filling of the central bulge with condensate after an initial condensation at the two surrounding necks (Fig. 1(a)); the second one refers to the filling of a remaining adjacent throat via a liquid-vapor meniscus advancing from the bulge (Fig. 1(b)). This second phenomenon is called *advanced adsorption* (Esparza et al., 2004) and emerges if the sizes of the central cavity and its delimiting necks fulfill certain ratios. Given this circumstance, the following sequence can ensue: first, vapor condensation happens at the smaller of the two delimiting necks; next the central cavity fills with condensate (once the vapor pressure attains a critical value); finally the remaining empty neck is trespassed right away by the advancing liquid-vapor meniscus coming from the bulge. During the development of the ascending boundary isotherm, advanced adsorption causes the liquid filling of tubular pores at pressures smaller than those required for condensation to occur in isolated pores of similar characteristics. If interconnected voids possess comparable sizes, the advancing meniscus can trespass a sequence of adjacent pores thus possibly spreading over the whole network.

Delayed Adsorption

Vapor-filled necks surrounding a given cavity can create a *delayed condensation* in this latter void. This situation is likely to happen in pore assemblages consisting of a central cavity delimited by necks having sizes not too different from that of the cavity. Imagine, for instance, that a set of two cylindrical pores surround a nearly spherical cavity (see Fig. 1(b)), if the size of this bulge is smaller than twice the size of anyone of its surrounding throats (and assuming that condensation is dictated by the classical Kelvin equation) then the cavity will only be filled with condensate if a continuous meniscus is formed around this pore. This situation will just happen if at least one of the surrounding necks is being filled with condensate (Mayagoitia et al., 1985), i.e. the central cavity will be condensate-filled at a pressure larger than that required if this bulge existed isolated from other pores.

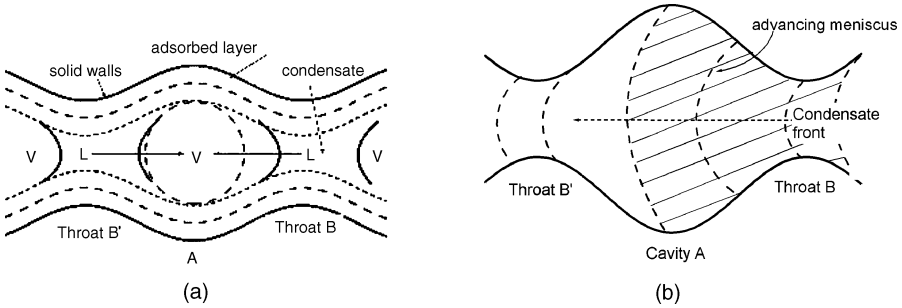

Figure 1. (a) Vapor condensation around the central cavity of a tubular pore after menisci are formed at the two delimiting throats. (b) Liquid invasion (advanced condensation) of throat B' after the filling of the central cavity. L = liquid, V = vapor.

Construction of Simulated 3-D Porous Networks and Morphological Details

Details about the method of construction of 3-D porous networks through Monte Carlo simulation can be found elsewhere (Cordero et al., 2001); similarly, the algorithm that is employed to replicate sorption processes in porous networks has been reported somewhere else (Rojas et al., 2002). The conditions required for cavities (hollow spheres) and necks (hollow cylinders open at both ends) to be fully occupied by either condensate or vapor are calculated by means of the Broekhoff-de Boer equation (Broekhoff and de Boer, 1967), while the thickness of the adsorbed film is approximated via the Harkins-Jura equation (Harkins and Jura, 1944). Here, we present results related to two extreme kinds of porous substrates: Networks I and II (abbreviated as N-I and N-II). N-I represents a case of high correlation existing among the sizes of cavities and their delimiting necks; in this system the mean connectivity C is equal to 2 (i.e. each spherical cavity is delimited, in average, by two cylindrical capillaries). On the other hand, N-II involves a constant connectivity equal to 6. The pore-size distributions of cavities and necks have been both chosen as Gaussian. Statistical parameters of the dual pore-size distributions are summarized in Table 1. In both cases, most pore diameters are larger than 50 Å so that a good accuracy (for finding out the thermodynamic conditions at which phase transitions occur) is expected through the use of the Broekhoff-de Boer eqn. Under all the above circumstances, the expectancy is to observe a strong process of advanced adsorption occurring in N-I and a definite phenomenon of delayed adsorption taking place in N-II.

Topological properties of N-I and N-II have been previously described in detail (Cordero et al., 2001). Particular characteristics of N-I and N-II are as follows. The very similar mean diameter sizes of cavities and throats in the case of N-I is the cause of a strong size correlation between these two kinds of void elements and the network structuralizes in the form of long tubes (cavities and throats coalesce together forming long straight cylinders) that sometimes meet with homologous capillaries at intersecting points (manifold connections). In turn, N-II substrate consists of spherical hollows delimited by cylindrical necks; the sizes of the necks are just the right ones to accommodate six tubes around the cavities; the sizes of the throats although smaller than those of cavities are however not excessively different. Despite their topological differences, networks N-I and N-II share a common property: pores in these two substrates group in a patchwise fashion according to their sizes. In other words, distinctive pore regions appear: large cavities are connected to big necks, medium size cavities are linked to intermediate size throats, and finally small cavities are joined to small necks. Briefly speaking, N-I is a multiplex system of long tube-like pores while N-II comprises interconnected manifold arrangements of cavities and throats.

Table 1. Statistical parameters of simulated porous networks. $\bar{R}_B$ and $\bar{R}_S$ are the mean radii of necks and cavities, respectively; σ_B and σ_S are the standard deviations; C is the mean connectivity; Ω is the overlap.

Network	$\bar{R}_B$/Å	$\bar{R}_S$/Å	σ_S, σ_B/Å	C	Ω
N-I	55.5	57.5	8	2	0.9
N-II	52	82	8	6	0.2

Adsorption Results

Delayed and advanced adsorption will be evidenced through the comparison between actual and calculated pore-size distributions (PSD) proceeding from boundary and primary scanning N_2 sorption isotherms at 77 K simulated on the N-I and N-II networks. PSD functions are estimated via the BJH method while employing the Broekhoff-de Boer eqn. for predicting the conditions at which phase transitions are going to take place in the pores (Ojeda et al., 2003). Simplified interfacial geometries, i.e. cylindrical and hemispherical, will be assumed throughout this work for predicting these phase transitions or describing menisci displacements. The determination of primary scanning curves will provide further valuable information for unveiling advanced or delayed adsorption processes.

N-I Analysis

Boundary Curves. PSD functions are determined from the simulated ascending boundary (AB) and descending boundary (DB) curves depicted in Fig. 2(a). Several aspects are worth mentioning (see Fig. 2(c)). First, the calculated PSD functions are quite different from the precursory Gaussian distributions. Second, although rather misleading if compared to actual distributions, the PSD curves calculated from the AB

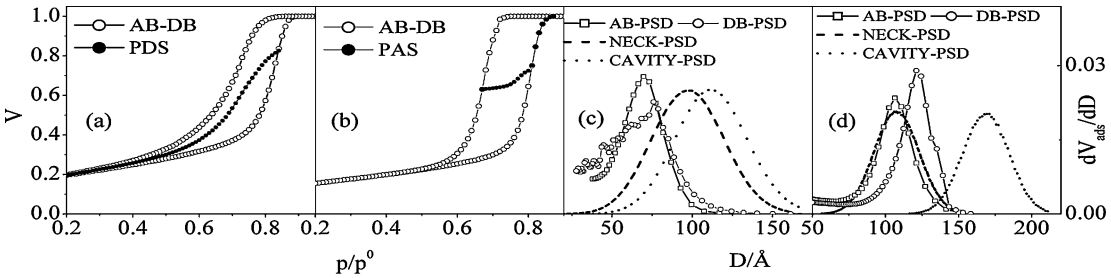

Figure 2. Isotherms and PSD functions of N-I and N-II substrates.

and DB curves are not too different from each other (Fig. 2(c)). This can be attributed to the topology of N-I, i.e. an interconnected multiplex arrangement of tube-like pores. The AB- and DB-PSD curves render pore sizes smaller than the real ones, this behavior hinting towards the existence of advanced adsorption (therefore explaining the deceptive AB outcome) as well as of pore-blocking (accounting, in turn, for the misleading DB result). The proximity between the AB-PSD and DB-PSD curves suggests the involvement of hemispherical menisci during the development of both paths, therefore pointing towards the irruption of advanced adsorption (displacement of hemispherical menisci) and pore-blocking effects (hemispherical interfaces located at pore mouths block the access to the vapor phase). A concluding remark is that pores of the N-I substrate are far from constituting independent pore domains.

Primary Descending Scanning (PDS) Curves. A clearer insight about the irruption of advanced adsorption in N-I can be perceived by comparing the appearances of the PSD functions obtained from the AB and PDS curves (Fig. 2(a)), respectively. For instance, if the development of the adsorption process on N-I occurred freely of the latter phenomenon, then the PSD curves corresponding to AB and PDS isotherms should overlap over the whole interval of pore sizes consistent with the amount of voids that remain empty up to the point of reversal of the scanning curve. The PSD functions evaluated from the AB and PDS curves are depicted in Fig. 3(a). Here, it can be seen that these PSD curves diverge in an apparently strange way: the PDS path renders pore sizes larger than those proceeding from the AB curve. Let us now discuss the possibility that the phenomenon of advanced adsorption can account for these particular PSD shapes. First, let us note that the AB-PSD curve is cut at a certain pore value that corresponds to the point of reversal of the PDS curve (Fig. 2(a)). Now, let us remember that our N-1 network is a multiplex system of tubular pores that meet at some manifold distribution points (Cordero et al., 2001). Let us now pass to the mechanistic aspects of the sorption process. Imagine that the smallest of the capillaries coinciding around a manifold connection is being filled with condensate (i.e. a cylindrical film is formed first on the walls of this capillary and later destabilized at certain relative vapor pressure). This condensation event could then be the cause by which hemispherical menisci start moving into the assembly of remaining empty tubes; the manifold joint will just act as a repartition point for menisci movements. The overall result is that a considerable amount of tubes are filled at pressures lower than those predicted by an independent pore behavior. Hence, the reason by which the PDS-PSD curve is located to the right of the AB-PSD function is a consequence of the fact that (along the AB path) some of the pores have been filled at lower pressures than those expected from an independent pore system, i.e. pore sizes are being underestimated (sometimes as much as 50%). Let us further clarify this point by assuming that a given pore has just suffered of advanced adsorption at some stage during the adsorption process leading to the point of reversal of the PDS curve; here a hemispherical meniscus has been formed and the pore has been completely flooded with condensate. Now think about desorption of condensate from this very same pore along the PDS path: in the absence of pore blocking (this event will be more likely as the point of reversal is located at lower pressures) desorption will then occur at the same relative pressure as that allowed for liquid invasion (i.e. the same hemispherical meniscus reappears once more in this pore). Thus, there arise two extreme possibilities: one is that a void can be filled and emptied reversibly, the other one is that a pore can be filled as if it were an isolated pore. These possibilities explain the partial overlap between AB- and PDS-PSD curves.

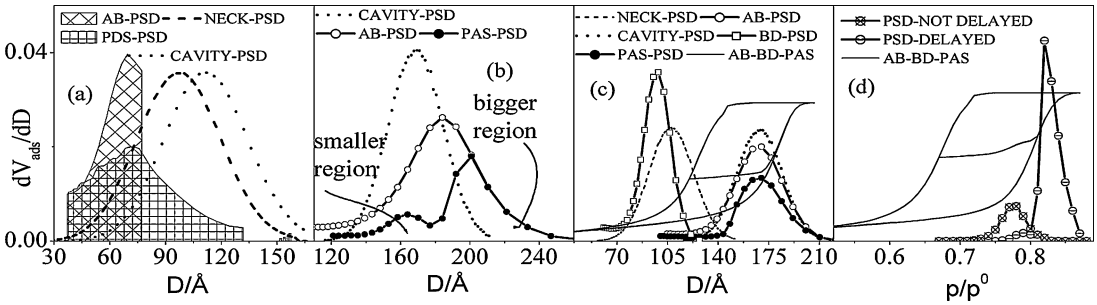

Figure 3. (a) PSD functions obtained from a PDS curve measured on N-I. (b)PSD curves corresponding to AB and PAS paths traced on N-II. (c) PSD functions from AB and PAS curves after decreasing by 20 Å the sizes of all necks. (d) Identification of cavities filled by delayed adsorption and in the absence of this process; the corresponding isotherms are also shown.

N-II Analysis

Boundary Curves. N-II depicts two rather distinctive PSD curves associated to the AB and DB isotherms (Fig. 2(d)). Let us first remember that this sample consists of interconnected spherical cavities, each one surrounded by six cylindrical necks. The sizes that were assigned to throats and cavities in the N-II sample suggest the following sorption mechanisms that help explaining the position and shapes of the PSD functions. Many (but not all) throats fill independently of any other pore element by means of a cylindrical meniscus, therefore the AB-PSD curve is very close to the actual neck distribution. On the other hand, cavities in order to be filled by condensate should await the formation of a continuous spherical meniscus inside them, i.e. C or at least C-1 of their peripheral bonds must contain condensate before vapor can start condensing in the cavity in question. Since at a given pressure along the AB isotherm not all throats are already filled with liquid, cavities are delayed in being occupied by condensate. This delayed condensation can be evidenced by calculating the PSD from the AB isotherm (spherical interface) (Fig. 3(b)); this AB-PSD result renders pore sizes somewhat larger than the actual PSD of cavities.

Let us now perform the following procedure that will wipe out the delayed adsorption phenomenon: each neck diameter in the N-II substrate will be decreased by 20 Å, the cavity sizes remaining unchanged. In principle, and because of the new characteristics of the dual PSD function, this action would eliminate the prospect of delayed adsorption. The new PSD functions calculated from the AB (spherical menisci) and DB (cylindrical interfaces) are shown in Fig. 3(c). Although the DB-PSD is not overlapping as well as before with the actual bond distribution, the new AB-PSD outcome fits the real one more accurately; delayed adsorption has then been precluded. The fit of the DB-PSD curve with the real distribution is not complete given that some pore-blocking is now occurring.

Primary Ascending Scanning (PAS) Curves. Valuable inferences about the incidence of delayed adsorption and the prospect of identifying the amount of cavities suffering of this phenomenon can be provided by the analysis of PAS curves. The PSD function, assuming hemispherical menisci, corresponding to the PAS curve in Fig. 2(b) is depicted in Fig. 3(b). This curve consists of two regions. The more extended one involves large pore sizes (Fig. 3(b)) while the other one is shifted toward lower sizes. This latter region seems to be linked to cavities which are filled without delay, while the large pore zone involves cavities filled through delayed adsorption. To further clarify this issue, the following experiment was carried out. Two PSD functions were directly evaluated during the simulation of the PAS sorption process: the first PSD depicts cavities filled with delay while the second PSD is linked to cavities filled without delay. This experiment could be easily performed through our simulation process by identifying those pores related to the two kinds of cavity filling during the development of the PAS curve. Both types of cavity distributions (delayed and non-delayed) were plotted as a function of the relative pressure in Fig. 3(d), then recreating the effect seen before in Fig. 3(b): the PAS-PSD consisted of two regions. Finally, a comparison was made between two PSD curves: one associated to the AB isotherm vs. another proceeding from the neck-size decreased network. Fig. 3(c) shows how the shape of the PAS curve is modified while its associated PSD lacked the two sections shown in Fig. 3(b), then rendering accurate

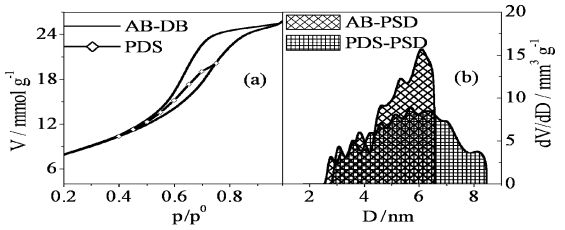

Figure 4. Experimental results found in a SBA-15 substrate: (a) Sorption isotherm, and (b) PSD function.

PSD values of cavities. Hence, a comparison between PSD's obtained from AB and PAS curves constituted an efficient tool for detecting delayed adsorption.

Relationship of Theoretical Findings with Experiment

A qualitative comparison was made between the results found above and some experimental data (Esparza et al., 2004). Figure 4 presents the PSD of a SBA-15 sample along with the corresponding isotherm. It is evident the similarity between Figs. 3(a) and 4(b). Advanced adsorption can also explain the PSD shapes found in Fig. 4(b). Experimental confirmation of delayed adsorption is still waiting for suitable porous substrates.

Conclusions

Simulated porous networks showing delayed and advanced adsorption have been built by a Monte Carlo method. Delayed adsorption is evidenced by comparing the PSD outcomes of AB and PAS curves; on the other hand, advanced adsorption is confirmed by comparing PSD functions obtained from AB and PDS isotherms. The AB shape can be highly influenced when the sizes of adjacent pores are highly correlated.

Acknowledgment

Thanks are given to CONACyT (México)-CONICET (Argentina) for financing the joint Project "Catalysis, Fisicoquímica de Superficies e Interfases Gas-Sólido".

References

Androutsopoulos, G.P. and C.E. Salmas, "A New Model for Capillary Condensation-Evaporation Hysteresis Based on a Random Corrugated Pore Structure Concept: Prediction of Intrinsic Pore Size Distributions. 1. Model Formulation," *Ind. Eng. Chem. Res.*, **39**, 3747–3763 (2000).

Broekhoff, J.C.P. and J.H. de Boer, "Studies on Pore Systems in Catalysts. IX Calculation of Pore Distributions from the Adsorption Branch of Nitrogen Sorption Isotherms in the Case of Open Cylindrical Pores. A. Fundamental Equations," *J. Catalysis*, **9**, 8–14 (1967).

Cordero, S., F. Rojas, and J.L. Riccardo, "Simulation of Three-Dimensional Porous Networks," *Colloids and Surfaces A: Physicochem. Eng. Aspects*, **187–188**, 425–438 (2001).

Esparza, J.M., M.L. Ojeda, A. Campero, A. Domínguez, I. Kornhauser, F. Rojas, A.M. Vidales, R.H. López, and G. Zgrablich, "N_2 Sorption Scanning Behavior of SBA-15 Porous Substrates," *Colloids and Surfaces A: Physicochem. Eng. Aspects*, **241**, 35–45 (2004).

Everett, D.H., "Thermodynamics of Multiphase Fluids in Porous Media," *J. Colloid Interface Sci.*, **52**, 189–198 (1975).

Harkins, W.D. and G. Jura, "Surfaces of Solids. XII. An Absolute Method for the Determination of the Area of a Finely Divided Crystalline Solid," *J. Amer. Chem. Soc.*, **66**, 1362–1366 (1944).

Mayagoitia, V., F. Rojas, and I. Kornhauser, "Pore Network Interactions in Ascending Processes Relative to Capillary Condensation," *J. Chem. Soc., Faraday Trans 1*, **81**, 2931–2940 (1985).

Neimark, A.V., "The Method of Indeterminate Lagrange Multipliers in Nonlocal Density Functional Theory," *Langmuir*, **11**, 4183–4184 (1995).

Ojeda, M.L., J.M. Esparza, A. Campero, S. Cordero, I. Kornhauser, and F. Rojas, "On Comparing BJH and NLDFT Pore-Size Distributions Determined from N_2 Sorption on SBA-15 Substrata," *Phys. Chem. Chem. Phys.*, **5**, 1859–1866 (2003).

Ravikovitch, P.I., D. Wei, W.T. Chueh, G.L. Haller, and A.V. Neimark, "Evaluation of Pore Structure Parameters of MCM-41 Catalyst Supports and Catalysts by Means of Nitrogen and Argon Adsorption," *J. Phys. Chem. B*, **101**, 3671–3679 (1997).

Rojas, F, I. Kornhauser, C. Felipe, J.M. Esparza, S. Cordero, A. Domínguez, and J.L. Riccardo, "Capillary Condensation in Heterogeneous Mesoporous Networks Consisting of Variable Connectivity and Pore-Size Correlation," *Phys. Chem. Chem. Phys.*, **4**, 2346–2355 (2002).

Sarkisov, L. and P.A. Monson, "Hysteresis in Monte Carlo and Molecular Dynamics Simulations of Adsorption in Porous Materials," *Langmuir*, **16**, 9857–9860 (2000).

Vishnyakov, A. and A.V. Neimark, "Monte Carlo Simulation Test of Pore Blocking Effects," *Langmuir*, **19**, 3240–3247 (2003).